PB 161591

NBS

Technical Note 90

FLUX SWITCHING MECHANISMS IN FERRITE CORES AND THEIR DEPENDENCE ON CORE GEOMETRY

U. S. DEPARTMENT OF COMMERCE
NATIONAL BUREAU OF STANDARDS

THE NATIONAL BUREAU OF STANDARDS

Functions and Activities

The functions of the National Bureau of Standards are set forth in the Act of Congress, March 3, 1901, as amended by Congress in Public Law 619, 1950. These include the development and maintenance of the national standards of measurement and the provision of means and methods for making measurements consistent with these standards: the determination of physical constants and properties of materials; the development of methods and instruments for testing materials, devices, and structures; advisory services to government agencies on scientific and technical problems; invention and development of devices to serve special needs of the Government: and the development of standard practices, codes, and specifications. The work includes basic and applied research, development, engineering, instrumentation, testing, evaluation, calibration services, and various consultation and information services. Research projects are also performed for other government agencies when the work relates to and supplements the basic program of the Bureau or when the Bureau's unique competence is required. The scope of activities is suggested by the listing of divisions and sections on the inside of the back cover.

Publications

The results of the Bureau's work take the form of either actual equipment and devices or published papers. These papers appear either in the Bureau's own series of publications or in the journals of professional and scientific societies. The Bureau itself publishes three periodicals available from the Government Printing Office: The Journal of Research, published in four separate sections, presents complete scientific and technical papers; the Technical News Bulletin presents summary and preliminary reports on work in progress; and Basic Radio Propagation Predictions provides data for determining the best frequencies to use for radio communications throughout the world. There are also five series of nonperiodical publications: Monographs, Applied Mathematics Series, Handbooks, Miscellaneous Publications, and Technical Notes.

Information on the Bureau's publications can be found in NBS Circular 460, Publications of the National Bureau of Standards ($1.25) and its Supplement ($1.50), available from the Superintendent of Documents, Government Printing Office, Washington 25, D.C.

NATIONAL BUREAU OF STANDARDS

Technical Note

90

MAY 1961

FLUX SWITCHING MECHANISMS IN FERRITE CORES AND THEIR DEPENDENCE ON CORE GEOMETRY

George William Reimherr

DISTRIBUTED BY

UNITED STATES DEPARTMENT OF COMMERCE

OFFICE OF TECHNICAL SERVICES

WASHINGTON 25, D. C.

Price $1.25

TABLE OF CONTENTS

LIST OF FIGURES

FLUX SWITCHING MECHANISMS IN FERRITE CORES AND THEIR DEPENDENCE ON CORE GEOMETRY

by

George William Reimherr

ABSTRACT

Plots of reciprocal switching time against applied magnetic field for ferrimagnetic or ferromagnetic cores usually show two or three interconnecting straight line segments. Different theoretical flux reversal mechanisms have been proposed for each segment. Descriptive models of these mechanisms are presented. Switching curves are shown for seven ferrite cores of different composition, and for a ferromagnetic tape core. The inverse slope of the switching curve known as the switching coefficient, was calculated for these cores and it is shown to agree well with values given by other experimenters and by theory.

Experiments were made to ascertain whether the flux reversal mechanisms are affected by core geometry. Nine ferrite cores were separated into four groups. The cores of each group had identical chemical composition and originally had nearly equal cross sections and identical switching curves. The cores of each group were then ground into different cross sections, at least one being rectangular and the other being square or circular, and switching curves were again taken of these cores. No effect of geometry upon the flux reversal mechanisms was found. Several factors which may affect the switching coefficient are given.

SECTION I

INTRODUCTION

The mechanism of rapid magnetic flux reversal has received considerable attention both because of its intrinsic importance in understanding the behavior of ferromagnetic and ferrimagnetic materials, and because of the desire to decrease the time required to store or to retrieve information in magnetic memory systems of electronic computers. The cores used in magnetic memory systems are generally of ferrite materials having rectangular d. c hysteresis

loops characterized by steep sides and almost flat tops. It is with this type of ferrite that this investigation is most concerned.

A relation found to hold when ferrite cores, metallic ribbon cores, or thin films are subjected to sufficiently high current pulses of short duration is the switching equation of Menyuk and Goodenough (1),

$$(H - H_o)\tau = S_w \qquad (1)$$

in which

- H = the applied magnetizing force
- H_o = the projected threshold magnetizing force when switching the core in a given mode
- τ = the switching time. It is defined in the present investigation as the duration of electrical pulse needed to switch irreversibly 90% of the flux that is switched irreversibly when completely reversing the magnetic state
- S_w = the switching coefficient, a constant over a restricted range of applied field

The above-mentioned equation can be put into another form; namely,

$$\frac{1}{\tau} = \frac{1}{S_w}(H - H_o) \qquad (2)$$

Hence, a plot of reciprocal switching time against applied magnetizing force should yield a straight line with a slope equal to the reciprocal of the switching constant. However, if the range of applied field is extended sufficiently, one may obtain three connecting lines for a ferrite, each having a different slope. This suggests that different modes (or mechanisms) of flux reversal are dominant over various regions of the switching curve.

Various models have been proposed to account for these switching mechanisms.[1], [4], [8]. The model of flux reversal for the lowest region of field intensity corresponds to that of domain wall motion.

At higher regions of field intensity, a model corresponding to an incoherent rotation of the electronic spins is proposed while at still higher field intensities, a model corresponding to a coherent rotation of electronic spins has been presented.

A short discussion of each of the three models for flux reversal will follow. It is interesting to note that these models apply as well to the flux reversal mechanisms in metallic ribbon cores and thin films as they do to ferrite cores. While the model of domain wall motion seems to be generally accepted, one is cautioned that the flux configuration considered in the rotational models should not be considered as an exact description of the actual flux reversal process.

SECTION II

MODELS OF FLUX REVERSAL

Domain Wall Motion. The existence of regions within a ferromagnetic or ferrimagnetic substance in which all the net electronic magnetic moments are essentially aligned, has been fairly well established. These regions are called domains. A magnetic material when in the un-magnetized state may be composed of very many of these domains, the magnetization vectors within different domains being in different directions so that there is no over-all magnetization exhibited by the material.

Adjacent domains are separated by transition regions within which the magnetization gradually changes direction from that of one domain to that of the adjacent domain. These regions of transition are called "domain walls" or "Bloch walls". In iron, a Bloch wall is of the order of 10^{-4} mm thick, corresponding to several hundreds of inter-atomic spacings; a domain itself may be of the order of 0.001 to 0.1 mm.

When a magnetic material is initially subjected to an external magnetic field whose amplitude equals or exceeds somewhat the coercive force of the material, those domains which happen to be

favorably oriented with respect to the external field will grow at the expense of the neighboring domains by virtue of movement of domain walls. When the specimen is completely saturated in the direction of the applied external field, the moving domain walls which brought about this situation have been annihilated, either by combining with other walls or by running off the edge of the grain.

Now suppose the external field "H" is reduced to zero and then is given some small value in the reverse direction sufficient to initiate flux reversal in the specimen. For flux reversal by domain wall motion, it is necessary for domains of reversed magnetization to form; i.e., to be "nucleated". If the specimen were a perfect single crystal, this would require extremely high fields, due to the strong internal anisotropy fields which supply a torque opposing such change. However, imperfections in the actual specimen give rise to internal fields which allow nucleation of reverse magnetization at much lower values of applied field. Any commercial magnetic material will have many nuclei for the formation of domain walls such as crystal boundaries, lattice defects, and surface irregularities.

In general, domains of reverse magnetization form as H is lowered from $+H_{maximum}$ to $-H_{coercive}$. A requirement for a rectangular B-H loop is that no nucleation take place as H decreases from H_{max} to $-H_{coercive}$ (1). Once the walls are nucleated at points of crystal imperfection, they find themselves tied down by these same imperfections so that it takes a finite applied field in the reverse direction to break the fields away from the imperfections. Thus imperfections are responsible for low coercive forces as they nucleate domains of reverse magnetization; however, they keep the coercive force from being zero by stabilizing the domain walls.

The average velocity of the domain walls when the external field equals the coercive force is about zero. If the external field exceeds the coercive force, the domain walls are thought to accelerate very rapidly to an average velocity which is maintained

until the walls collide with one another or with a grain boundary.

Damping of the motion of the domain walls arises from two factors. The first factor is the presence of eddy currents. This factor is of no practical consequence in ultra-thin metallic tapes of 1/8 mil thickness, or in commercial ferrites since their resistivity is typically of the order of 10^5 ohm cm. The second cause of damping is the relaxation contribution which arises from the delayed response of the atomic spins to a force which would change their direction; it is an inherent quality of the magnetic material (1).

An expression for the domain wall velocity v is given in reference (2) as

$$v = \frac{4\gamma A(H-H_{o1})}{\sigma a} \qquad (3)$$

where

γ = magneto mechanical ratio of the electron
A = exchange factor (10^{-6} erg/cm for ferrites)
σ = wall energy (about 1 erg/cm^2 for most ferrites)
a = a damping constant, obtained in microwave resonance experiments

If a domain has an average initial width d, then the reversal time τ will be the time it takes the walls to go a distance d/2. It follows that

$$S_{w_1} = \tau(H - H_{o_1}) = \frac{\sigma d a}{8\gamma A} \qquad (4)$$

This is not the only expression for S_{w1} present in the literature. One may refer, for example, to reference (3) or (4). All three expressions, however, have in common the fact that S_{w1} is proportional to the product of the distance a domain wall moves, and the damping constant. It appears to be generally accepted, today, that at low values of external drive fields, flux reversal occurs by domain wall motion.

Incoherent Rotation. As the external drive field continues to increase above the coercive force, a break in the switching curve is noted, followed by a straight-line region for intermediate values of drive field. In this region of drive field, it is thought (4) that a switching process by incoherent rotation more nearly agrees with experiment than does the domain wall motion model.

If flux reversal occurs by domain wall motion, then intuitively, one might expect S_w to be quite sensitive to the structure of the ferrite, since it is proportional to d, the average distance a wall moves before colliding with another wall. However, S_{w_2} (the switching constant for incoherent rotation) has been found to be relatively independent of the grain size or even of the ferrite used (4). A variation in grain size from 2 to 1500 microns, or a change in chemical composition between ferrites, and, if the 1/8 mil permalloy material is considered, a change from ferrimagnetic to ferromagnetic material, caused a variation in S_{w_2} by only a factor of three (4). This type of reasoning led to an abandonment of the domain wall motion mechanism in favor of an incoherent rotational model for the intermediate region of the switching curve.

A potential difficulty with any rotational model is that during flux reversal, large demagnetizing fields can result from the discontinuity of the magnetization at the boundary of the magnetic material. This implies that very large driving fields should be necessary for flux reversal by spin rotation; however, the experimental value of the projected threshold field is typically on the order of only a few oersteds (note for example H_{o_2} values in Table I). Hence, the incoherent rotational model must have the property that the demagnetizing fields can be neglected; this is attempted in the so-called "spiral" model (5).

To illustrate the spiral model, one may consider the toroid to be equivalent to an infinite cylinder extending along the Z axis (5). Let the external field H be applied along the negative Z direction,

and let the magnetization M be in the partially switched state so as to make an angle θ with the Z axis. See Figure 1. The angle θ varies only with time, during which flux reversal occurs.

The magnetization vector does not point uniformly in any one direction during flux reversal, but instead is presumed to form a spiral pattern around the Z-axis as shown in Figure 1. This in turn results in the appearance of poles of alternating sign at the boundary of the cylinder. The surface poles form a helical pattern with a spacing λ. If λ is much smaller than the diameter of the cylinder, then the demagnetizing field due to the surface poles will be negligible throughout most of the volume of the cylinder (5). If one allows for the fact that there is a demagnetizing energy due to the surface poles and if an approximate expression for this energy can be found as a function of λ, then it is possible to find a value of λ which can minimize this energy. This expression for λ that minimizes the demagnetizing energy is given in the literature (5) as the following:

$$\lambda = 2\left(\frac{2\pi^2 RA}{M_s^2}\right)^{1/3} \qquad (5)$$

where

R = radius of cylinder
A = exchange constant, 0.15×10^{-6} ergs/cm for a manganese ferrite ($Mn_{1.4}Fe_{1.6}O_4$)
M_s = saturation magnetization in gauss

If one lets $R = 2.5 \times 10^{-2}$ cm, $M_s = 240$ gauss, one obtains $\lambda \approx 2.2 \times 10^{-4}$ cm, which is 2 orders of magnitude smaller than the assumed radius of the cylinder. Likewise, the fields due to the surface poles, when the pole density is at a maximum ($\theta = \pi/2$) are given (5) by the following expression:

$$H_Z = 2\pi M_s e^{-2\pi d/\lambda} \cos\left(\frac{2\pi}{\lambda}\right)Z \qquad (6)$$

where d is the distance from the surface. If $d \approx 3 \times 10^{-4}$ cm, the

fields have dropped to about 0.2 oersted. Hence, the influence of the demagnetizing fields is mainly limited to a surface layer having about 1/40 of the volume of the cylinder (5). A theoretical expression for the switching coefficient, as given by this model, is the following (4):

$$S_w = 2\alpha \left(1 + \frac{1}{\alpha^2}\right)\left(\frac{1}{\lambda}\right) A \qquad (7)$$

where

α = a damping constant taken from the Gilbert modification of the Landau-Lifshitz equation of motion for M_s (6)

λ = the gyromagnetic ratio

A = a term whose value depends on the remanent magnetization of the sample, and the definition of the switching time used. It is sometimes omitted because it usually is of the order of one (4).

It is not known with any certainty what value to choose for α in the above mentioned equation. However, assuming α to be the only variable, one can minimize S_w with respect to α, i.e., this would correspond to that value of S_w for the minimum switching time for a given externally applied magnetic field. Setting $\alpha = 1$, the minimum value for S_w in this switching mode is given by $4/\lambda$ or approximately 0.2 oersted-microseconds (oe-μsec). This value agrees with experiment, as will be seen later.

Coherent Rotation. A discussion of the existence of the very fast uniform rotational mode of switching of ferrite toroids appeared only recently in the literature (8). It was pointed out that a model for the rotational mode of switching of thin ferromagnetic film had recently been postulated (7) and had given a best explanation of the experimental observations (7) when large drive fields were applied along with a transverse magnetic field. An attractive postulate is that a similar mechanism of flux reversal could also apply to ferrite toroids. Since flux reversal in a thin film is easier to

visualize than it is for a ferrite toroid, a brief discussion of the coherent rotation model for a thin film will precede that for a toroid.

Consider a thin film with a uniaxial anisotropy in the plane of the sample. Let the external field be applied along the easy axis of magnetization. The magnetization in the film will then also line up in this direction. Now let the external magnetic field be reversed in sign, but still lie along the easy axis of magnetization in the sample. If the magnetization in the sample is to reverse by uniform rotation, then the magnetization of the whole sample can be represented as a single vector which rotates within the plane of the film. However, in the present situation, this cannot occur because the magnetization and applied field are colinear the initial net torque on the magnetization is zero. Hence, for sufficiently high fields, flux reversal must occur by the slower process of incoherent rotation in which it is assumed that the magnetization does not precess as a whole, but that the phase of the precession varies with position in the sample (7). This is similar to the incoherent rotation model for ferrite cores.

Consider the situation, however, if a small transverse magnetic field is applied along the plane of the film, but at right angles to the drive field and to the easy axis of magnetization. A small component of the magnetization now is at right angles to the external drive field. Now let the direction of the external drive field be reversed.

There is now a net torque causing the whole magnetization to revolve in a vertical direction. This creates a strong demagnetizing field which in turn causes the whole magnetization to revolve as a single vector within the plane of the film. The fast reversal process may therefore be interpreted physically as a precession of the magnetization in the plane of the film around this demagnetizing field (8). The switching process is shown in Figure 2.

With this background, the case for the ferrite toroid will now be presented as given in reference (8).

If high speed flux reversal is to occur in ferrite toroids, it appears that a flux configuration must be induced that gives rise to a demagnetizing field around which the bulk of the flux may process. For this purpose, the "helical mode" is presented. As was done for the incoherent rotation model, the case of the toroid shall be approximated by considering it to be a cylinder of infinite length.

Suppose one takes the thin film in Figure 2 and wraps it up to form a hollow cylinder; the flux lines have now become helical with the small radial component, as in Figure 3. One may superpose many such hollow cylinders of decreasing radii in order to obtain a solid cylinder. The flux configuration is therefore uniform in the sense that the magnetization components are independent of position in the cylindrical coordinate system (8).

The final step in visualizing the helical mode is to take into account the curvature introduced by wrapping up the thin film. As a result of rolling up the film, the outer surface is stretched and the inner surface is compressed, leading to a difference in the magnetic surface charge density. This difference is assumed to distribute between the two surfaces as volume charge in a way to obtain a radial, position-independent demagnetizing field.

The complete configuration for this model as given in reference (8) is therefore a cylinder in which most of the magnetization follows a helical path. However, there is a small spatially independent radial component. The discontinuity of the radial magnetization at the surface of the cylinder creates a uniform surface charge distribution, and a radial demagnetizing field arises within the cylinder from the surface layer. The demagnetizing field lines terminate on the volume charge of opposite sign which occurs because $\nabla \cdot M \neq 0$ in the cylinder. A flux configuration has been selected which leads to a uniform demagnetizing field because this is

the analog to the uniform rotational mode in thin films. Note that the model assumes no interaction between shells.

The helical model gives the following expression for the minimum value of the switching time:

$$t_{min} = \frac{6.9 \times 10^{-8} \text{second}}{(M_s H_e)^{1/2}} \qquad (8)$$

where

M_s = saturation magnetization of the ferrits
H_e = excess threshold field ($H-H_o$)

Inserting a typical value for M_s of 240 gauss, and allowing H_e = 1 oersted gives as the minimum switching time 4.5×10^{-9} second for ferrite cores with H_e = 1 oersted drive field (within the framework of this model); this would lead to a minimum switching coefficient of approximately .005 oersted-microseconds.

To test this flux reversal model, the authors of this model (8) fabricated a core in which a 3 mil platinum wire loop was embedded in the center of the cross-section of the core (Figure 4). Normally, no current flows in the embedded wire and the flux pattern would be perpendicular to the plane of this paper. But with a small current in the wire, a component of the magnetization forms a circular flux pattern concentric with the wire. This can be considered equivalent to the case of the thin film with a transverse field as well as a normal drive field. When all the flux assumes the circular pattern, then one has approximately the half-switched state of the helical mode (8).

Switching curves were taken for the core with and without current flow in the embedded wire, and a switching time definition was used which took into account the fact that the core was already half switched in the case of current flow in the embedded wire. A reduction in switching coefficient from 0.11 oe-μsec to 0.05 oe-μsec by applying this current seemed to be in qualitative agreement with that experienced by applying a transverse field to a thin film.

One may note, however, that the observed switching coefficient of 0.05 oe-μsec is still an order of magnitude greater than the minimum value of 0.005 oe-μsec given by the model. The authors of the model (8) explain this by observing that they assumed a damping coefficient in their derivation of minimum switching time corresponding to optimum damping, and that this may not be applicable to the real situation; also they point out that the switching coefficient decreases as the temperature increases, and that the theoretical minimum value of S_w may be approached as the Curie temperature of the ferrite is approached. They did not obtain experimental verification of this because so much flux switched reversibly as the Curie temperature was approached as to make obscure the meaning of switching time. They did point out that a minimum measured value of S_w for the uniform rotational model in thin films was reported as 0.01 oe-μsec in the literature (9).

A difficulty in the experimental verification of this model arose when it was observed that no induced voltage appeared on the wire embedded in the core when the flux reversal in the core was presumably by the helical mode. This implied that the dynamic flux configuration was not as simple as the proposed helical mode. The difficulty can be resolved by a modification of the helical mode. This is done by assuming that there can still be a coherent rotation in each of the concentric shells; however, the direction and angular velocity of the magnetization vector may vary from one shell to another (10). This could explain the observed lack of induced voltage on the embedded wire mentioned previously.

This completes the descriptive analysis of the various models for magnetic flux reversal. The interested reader may refer to any of the references cited previously, or to reference (11) for more information on the subject. The next section will show a practical experimental method to obtain switching curves for magnetic cores, consistent with the definition of switching time used in this investigation.

SECTION III

MEASUREMENT OF SWITCHING TIME AND APPLIED MAGNETIC FIELD

The experimental layout used in this investigation to measure the data used in calculating a switching curve for a core is shown in Figure 5. The electrical pulses necessary to switch the core are provided by two pulse generators. The write pulse is generated by a pulse generator having a risetime of the order of 1 millimicrosecond (mμsec). The read pulse reverses the magnetization in the core from that provided by the write pulse. It is provided by a pulse generator having a risetime of the order of 20 mμsec.

The write pulse generator provides a variable write current up to a little over 2 amperes. Different write pulse widths are provided by charging a coaxial cable delay line to a voltage, V_o. A relay then discharges the cable across the external load resistor, R. The step voltage appearing across the load resistor is of duration t_0, twice the delay time of the coax line. If R is made equal to Z_o, the characteristic impedance of the line, the voltage across R is $\frac{V_o}{2}$. The pulse width is given by (2),

$$t_0 = 2Z_oC1 = 21\sqrt{LC} \qquad (9)$$

where

C = capacitance/unit length
L = inductance/unit length
1 = length of cable

and this is controlled by adjusting the length of the line. Pulse lengths from 10.7 to 1075 mμsec were available. They had fixed lengths and hence had to be calibrated only once.

The read pulse length and amplitude were held constant and were set so as to insure the total flux reversal of the core during every read cycle. With the exception of the earliest cores examined, A-1, A-2, and A-3, this value was about 1.4 amperes amplitude and a

pulse duration on the order of 7 microseconds. This amplitude was the highest attainable with the Read pulse generator. It provided an average driving field of about 5-1/2 oersteds.

To ascertain what percentage of the core was switched, a sense wire was wound through the core. Whenever flux reversal occurred in the core, a voltage pulse appeared at the sense winding. This would go into an RC integrator which in turn was connected directly to the scope input.

The write pulses occurred at a rate of approximately 75 cycles per second, while the read pulses occurred at a considerably higher rate and were not synchronized with the write pulses. The scope sweep was triggered only by the read pulses.

The sequence of events is as follows: The core, being in the remanent state after a series of read pulses each of which is capable of saturating it, receives a write pulse which drives it away from remanence. No core signal is seen, however, because the scope is not triggered by write pulses. Then, the next read pulse completely reverses any flux switched by the write pulse, restoring the core to its initial state. The flux reversal in the core creates a voltage pulse in the sense winding. This voltage pulse then goes to an RC integrator network whose output appears on the scope because the scope is triggered by the read pulse. The output from the integrator is proportional to the volt-second area of the core output pulse. A direct comparison of integrator signal height to the maximum height (attainable by using a write pulse which is sufficient to fully reverse the magnetization in the core) gives the fraction of irreversible flux switched. There is a lower limit of integrator signal height below which it becomes very difficult to take accurate readings. In the present case, this was about 6 millivolts.

The integrator time constant, RC, was adjusted so that the ratio of RC to the core output pulse length which was integrated remained relatively constant for all cores in a given comparison. For all

ferrite cores examined in this investigation, this ratio ran between about 20 and 27 when 90% of the core was switched irreversibly, with the exception of the earliest set examined, cores A-1 through A-3 for which the ratio was about 11.

The flux reversal field H of the core switching curve can in theory be found by measuring the write voltage pulse across a known value of load resistance (53.3 ohms in this particular case) when 90% of the flux of the core switches irreversibly. However, a perfect current source is not available; some back e.m.f. is generated by the core. But since the internal impedance of the pulse generator is about the same as that of the termination (or load) resistor, only half the core voltage appears across the load resistor, and an evaluation for H should appear as follows:

$$H = \frac{n(V_m - 1/2\ V_c)}{Rl}$$

where

H	=	applied magnetic field switching the core
R	=	resistance (53.3Ω)
n	=	number of turns (4)
l	=	mean magnetic path length
V_m	=	voltage measured across R when core is not switching, but which could switch 90% of the core flux irreversibly
V_c	=	average voltage generated by core while switching by 90%

SECTION IV

EXPERIMENTAL VALUES OF SWITCHING COEFFICIENTS

Results Found by the Present Author. Shown in Figs. 6, 7, and 8 are the switching curves for 5 types of commercially available ferrites as well as for a ferromagnetic tape core. All curves were taken at room temperature, about 23°C. The ferrites are of the size listed in commercial literature as 50 mil O. D., 30 mil I. D. and 15 mil in height. The tape core consists of 8 wraps of 4-79 Molybdenum-permalloy ribbon, each wrap being 1/8 mil in thickness.

It is noted that each ferrite shows 3 straight line regions in its switching curve, presumably corresponding to the 3 switching mechanisms mentioned previously. The ferromagnetic tape core also shows 3 straight line regions, although the difference between the upper 2 line segments is so small that within experimental limits of accuracy, the predominant switching mechanism for the upper 2 regions is probably the same; namely, incoherent rotation.

Values of the switching coefficient, S_w, and the projected threshold field, H_o, were found from these plots and are listed in Table I. The subscript corresponds to the switching mode; e. g., S_{w_1} is the switching coefficient for flux reversal by domain wall motion, with H_{o_1} being the corresponding threshold field, etc.

Results Found by Other Investigators. A brief look at some values of switching coefficients as found by other investigators might prove informative, although any rigorous comparison is impossible because of the differences in chemical composition and (usually) the definitions of switching time. For reversal by domain wall motion, Table II gives an indication of the wide differences possible in S_{w_1} and H_{o_1}, with switching time being defined as that time which elapses during a half reversal of the magnetization (12). Table III shows values of S_{w_1} for the system $Mn_{(1+x)}\ Fe_{(2-x)}\ O_4$ with switching time being measured between the 10% and 90% output voltage points (3).

Table IV gives experimental values of switching coefficients corresponding to flux reversal by incoherent rotation. Switching time is defined as the time required for the reversed induction to increase from 10% to 90% of the total flux switched (4). Note in particular how close the values of S_{w_2} are to each other.

Another author (10), whose definition of switching time is the same as that of the writer, has measured the switching coefficient corresponding to flux reversal by incoherent rotation for a wide selection of ferrites. He found the switching coefficient to fall in the range 0.11 to 0.41 oe-μsec (10). He feels this compares favorably with the predicted minimum value of 0.2 oe-μsec.

Flux reversal of ferrites by coherent rotation has been reported so recently that little in the way of experimental values of the switching coefficient S_{w_3} is available. One author (10) did report, however, that he obtained switching coefficients in the range 0.04 to 0.20 oe-μsec at 23°C.

SECTION V

SHAPING OF FERRITE CORES

The previous discussion showed that values of the switching coefficient could be found which showed good agreement with those found, or proposed, in the literature. Of particular interest was the coherent rotational mode of switching, because of the extremely fast reversal times associated with it. It was decided to examine the possibility of whether the switching process, especially that involving the helical mode, might be affected by the geometry of the core. In particular, it was felt that the helical mode might be enhanced by a circular cross section in preference to, say, a rectangular cross section having an extreme length to height ratio.

There were certain constraints imposed in this investigation which limited the length-to-height ratios attainable. These constraints are the following:

The cores had to be available commercially, and hence, came in certain fixed sizes. Because H, on the average, is proportional to the quotient of magnetomotive force to mean magnetic path length, the smallest cores (as used in this investigation) required the least current to produce a given field.

Cores of larger diameter would have required a larger number of turns on the write winding than the 4 used with the smallest cores.

The resultant higher core impedance would have reduced the ability of the core driving circuit to function as a current source.

Ferrite cores are fragile and are easily cracked. This sets restraints on how thinly a core can be ground. In particular, it was found that reducing l_o in Fig. (9a) to less than 0.10 mm would probably result in a cracked core.

Lastly, sufficient core material has to remain to give a workable output signal.

Hence, the most extreme length to height ratios available were on the order of 1:3, as noted in Table V. It was hoped that this would be sufficient to show up any possible dependence of the flux switching mechanism on core geometry.

Figure 9a shows a typical core, as received commercially. To give an idea what the dimensions may be, the following readings were taken for a typical core of type F_4.

$$\text{I.D.} = 0.760 \text{ mm} \pm 1.2\%$$
$$l_o = 0.254 \text{ mm} \pm 3\%$$
$$h_o = 0.368 \text{ mm} \pm 2.4\%$$

Figure 9b shows the appearance of a core ground into a square cross section of a given cross sectional area. By this method, the cores in Table V were fashioned. There are 4 sets of cores. The set into which a core belongs is noted by a capital letter between A and D such as A-1, C-2, etc. The length and height of each core cross section is given, as well as the ratio of height to length.

The uncertainties in measurement, shown in %, are actually a sum of 2 uncertainties. The first reflects the fact that the core may be thicker than average in one place, and thinner than average somewhere else. The second reflects an uncertainty in the absolute determination of a given dimension, due to uncertainty in focusing, slightly irregular core edges, etc.

SECTION VI

ERRORS OF MEASUREMENT

Errors in H. The errors in H involve measurement of the switcning current and the mean path length. The former involves measurement of voltage and resistance; the latter involves physical measurement of the core and a knowledge of the flux distribution of a partially switched core.

Voltage measurement uncertainties involve back e.m.f. correction, vertical deflection linearity, and visual error. Had no correction been made for the core's back e.m.f., a 5% error in H could have resulted; however, this correction was made, reducing the estimated error to $\pm 1/2\%$.

Voltage readings had to be taken directly from an oscilloscope trace which was calibrated from a unit which in turn was calibrated from a standard cell. Error estimate in vertical deflection linearity is $\pm 1/2\%$. Visual errors include errors in precision as well as systematic error, as for example, the finite width of the scope trace. The systematic error is believed $\leq$ 1%. To estimate the precision, each point of the switching curve of a typical core (C-2) was experimentally examined five times. The average voltage reading for each point was found, along with the standard deviation. The errors corresponding to a 95% confidence level were found by use of the Student t factor. Three of the 21 points had the maximum spread, about 1.5%. However, if all points for all cores are considered, there is really no preferred point for precision along the switching curve. Therefore, the $\pm 1.5\%$ spread was used for all points for all

cores. Therefore, visual error in voltage readings should be $\leq |\pm 2\ 1/2\%|$. A consequence of the definition of switching time is that part of the error in precision shows up also as an error in τ since it represents uncertainty in choice of the 90% flux reversal point.

The series resistor was checked on an impedance bridge against a standard resistance of equal value and known error. Both readings coincided. Therefore, error in resistance is assumed $\leq |\pm 1/2\%|$.

Many readings were taken of core measurements. It was found that both the inside and outside diameter of a typical core may vary by $\pm 1/2\%$ from its average value. It is felt that a reasonable value of the uncertainty in path length due to uncertainty in core measurement is $\leq |\pm 1\%|$.

Flux distribution in a partially switched core presumably varies with the speed of flux reversal. Were the d.c. hysteresis loop applicable, then a 90% switched core would have practically all of the flux reversed within the inner 90% of the core, the outer 10% remaining virtually untouched. This was the reasoning used in this work too. The other extreme is that the whole core could switch 90%. Perhaps, considering the high frequencies involved, the true distribution is somewhere between those 2 extremes, leading to an additional uncertainty in path length of about +1% (path length too low, making H too high).

The total absolute error in H is estimated to be between +5% and -6% for the ferrite cores, and ±5% for the ferromagnetic tape core.

Errors in τ. There are two categories of error involved in the absolute determination of switching time τ. The first is direct and comes from the uncertainty in the absolute value of pulse lengths. The second source is indirect and comes from an uncertainty in estimating the 90% point of irreversible flux reversal, inherent in the definition of switching time. It is estimated that for the cores used in this investigation, a 1% error in estimating the 90% point can result in a 4% error in τ.

There are 21 different pulse lengths used in this investigation. Those $\geq$ 96.75 mμsec were measured visually; those less than that were measured by integrating their volt-second output and comparing their integrated height maximum with that of a known pulse length. Hence, they acquired the error in the known pulse length also. All readings were taken five times, and the deviations from the average value were adjusted to provide a 95% confidence level. The scope sweep calibration was made with a signal generator which in turn was calibrated against the signal broadcast by radio station WWV. A typical spread in the absolute determination of a short pulse length is about ±3%; it drops below 1% for pulse lengths > 100 mμsec.

There are several uncertainties in estimating the 90% flux reversal point. All concern the integrator response to the core output signal. All errors are small because the readings were taken in a comparative sense--the 90% flux reversal integrator signal amplitude compared with that of 100% flux reversal.

The uncertainty due to visual observation is believed to be ±1/2%; that due to vertical deflection linearity, $\leq |\pm 1/2\%|$; that due to the imperfect integrator, about +1/2%; i.e., the 89.5% flux reversal curve was probably found instead of the 90% curve, due to the imperfect integrator. Any error due to capacitor leakage ($C \approx 53$ μμf) was neglected.

Although the estimated error in determining the 90% flux reversal point is only -1% to + 1 1/2%, the corresponding likely error in τ is -4% to +7% for each point in the graphs. It is seen that this is a larger source of error in τ than is the absolute determination of the pulse lengths.

Error in Comparative Measurement. The cores of sets A to D were made in such a way that the cross sectional area, hence the core output signal of each core in a set, was nearly equal. Also, the ratio of integrator RC time constant to core output signal duration was kept practically the same for each core of a set. Therefore, the

comparative error between the cores of a set is small, being composed only of precision error (±1.5%), uncertainty that the cores of a given set originally had identical switching curves (±1/2%), and uncertainty in flux distribution (-0.4% for the core with the larger mean path).

SECTION VII

RESULTS AND CONCLUSIONS

Before being ground into their various special shapes, all cores of a given set were similar in dimension and in chemical composition and gave identical switching curves. After being ground into their various final shapes, the switching curves of each core of a given set were again taken and compared between members of the same set. The results are shown in the switching curves of Figures 10 through 13. The estimated comparative error for each point in these plots lies between +2.0% to -2.4% of the H value of that point, in a direction parallel to the H axis. Since the switching curves of the cores of a set were already practically coincident, the comparative error was omitted for the sake of clarity. It is seen that, within the limits of comparative accuracy, the switching curves of all cores of a given set are identical.

The conclusion of the investigation is that within experimental limits, no effect of core geometry on the switching properties of the ferrite core types examined was found. This assumes that only cores having practically equal cross sectional areas, and hence similar core voltage waveforms, are used. If there is a dependence of switching mechanisms on core geometry, it evidently occurs rather suddenly rather than gradually, and it probably requires much more extreme shapes than those used in this investigation. Hence, the possibility of such a dependence has not been completely eliminated by the results of this investigation.

In conclusion, a listing of items which have been thought to influence the switching coefficient, S_w, could include the following:

1. chemical composition - this is noted in Tables I through IV;

2. method of preparation - it is known that the grain size and the number of voids in the ferrite are affected by the sintering temperature and sintering time duration. One group of investigators (2) reported that for a ferrite composed of 35% MgO, 25% MnO and 40% Fe_2O_3, an increase in firing (sintering) time generally increased grain size, lowered the coercive force, but had little effect on S_w;

3. temperature - the switching coefficient is temperature dependent, and it generally lowers as the temperature increases. As an example, the value of S_{w_2} for the ferrite $Mn_{0.46}Mg_{0.71}Fe_{1.76}O_4$ was found (4) to be 0.46 oe-μsec, at 77°K, and only 0.18 oe-μsec, at 473°K. The Curie point for this ferrite was given as 550°K (4);

4. effect of core geometry - this writer has found no such effect on S_w, within the areas of constraint mentioned in section V;

5. definition of switching time - the absolute value of S_w obviously depends on what one uses as his definition of switching time, τ. Unfortunately, there are a number of ways that τ is defined in the literature, 3 of which were noted in conjunction with Tables II, III and IV. Perhaps in the future, a standard way to define τ can be agreed on by all investigators;

6. rise time of drive current pulse - a ferrite core can be switched faster with a pulse having a short rise time than with a pulse having a relatively long rise time, assuming a similar (peak) value of external drive field. At least one investigator (13) noted a decrease in the switching coefficient with a faster pulse rise time;

7. effect of previous history - not only is the switching rate dependent on the initial state of magnetization and the applied external field, but also on the method by which the core was brought to its initial state of magnetization. In particular, the core output voltage waveform is dependent on the drive field used to attain the initial remanent state (14).

SELECTED BIBLIOGRAPHY

(1) N. Menyuk and J. B. Goodenough, J. Appl. Phys. 26, 9(1955).

(2) Private Communication.

(3) T. J. Matcovich and C. J. Kriessman, J. Appl. Phys. 30, 36s (1959).

(4) E. M. Gyorgy, J. Appl. Phys. 28, 1011 (1957).

(5) E. M. Gyorgy, J. Appl. Phys. 29, 1709 (1958).

(6) T. L. Gilbert and J. M. Kelley, Proceedings of the Pittsburgh Conference on Magnetism and Magnetic Material, June 14-16, 1955. American Institute of Electrical Engineers, New York, 1955, p 253.

(7) F. B. Humphrey and E. M. Gyorgy, J. Appl. Phys. 30, 935 (1959).

(8) E. M. Gyorgy and F. B. Hagedorn, J. Appl. Phys. 30, 1368 (1959).

(9) C. D. Olson and A. V. Pohm, J. Appl. Phys. 29, 274 (1958).

(10) W. L. Shevel, J. Appl. Phys. 30, 47s (1959).

(11) E. M. Gyorgy, J. Appl. Phys. 31, 110s (1960).

(12) J. Smit and H. P. J. Wijn, Ferrites, John Wiley and Sons (1959), pp 341-343.

(13) B. R. Eichbaum, J. Appl. Phys. 31, 117s (1960).

(14) R. W. McKay and K. C. Smith, J. Appl. Phys. 31, 133s (1960).

Ferrite Symbol	Chemical Composition	S_w (oe - μsec)			H_o (oersteds)		
		S_{w_1}	S_{w_2}	S_{w_3}	H_{o_1}	H_{o_2}	H_{o_3}
F_1	(Mg-Mn-Zn-ferrite)	0.35	0.22	0.17	1.4	2.4	3.7
F_2	(Mg-Mn-Zn-ferrite)	0.39	0.26	0.20	1.7	3.0	5.1
F_3	(Mg-Mn-ferrite	0.30	0.26	0.19	3.5	4.0	6.0
F_4	(Mg-Mn-ferrite)	0.42	0.26	0.21	1.9	3.5	5.5
F_5	(Mg-Mn-Zn-ferrite)	0.38	0.24	0.18	1.5	2.5	4.0
4-79 permalloy	4%Mo; 79%Ni; 17%Fe	0.24	0.16	0.14	0.49	0.83	1.6

Table I. Switching Constants and Threshold Fields for the Switching Curves in Figures 6, 7, & 8.

Ferrite Chemical Composition	H_{o_1} oersted	S_{w_1} oe - μsec
$Mg_{0.45}Mn_{0.78}Fe_{1.77}O_4$	0.9	0.4
$Cu_{0.25}Mn_{0.75}Fe_2O_4$	0.85	0.4
$Mg_{0.6}Ni_{0.4}Fe_2O_4$	3.6	1.1
$Li_{0.47}Ni_{0.06}Fe_{2.47}O_4$	2	0.5
$MnFe_2O_4$	0.5	1.6
$Ni_{0.5}Co_{0.1}Fe_{2.4}O_4$	12	13
$Mn_{0.18}Co_{0.02}Fe_{2.8}O_4$	2.5	4
$Co_{0.1}Fe_{2.9}O_4$	8	50

Table II. Switching Coefficients S_{w_1} and Threshold Fields H_{o_1} (12).

Ferrite Chemical Composition	S_{w_1} oe - μsec
$MnFe_2O_4$	0.55
$Mn_{1.43}Fe_{1.57}O_4$	0.46
$Mn_{1.84}Fe_{1.16}O_4$	0.36

Table III. Switching Coefficients for the System $Mn_{(1+X)}Fe_{(2-X)}O_4$ (3).

Ferrite Chemical Composition	S_{w_2} oe - μsec
$Mn_{0.46}Mg_{0.71}Fe_{1.76}O_4$	0.25 to 0.35
$Zn_{0.39}Mn_{0.47}Mg_{0.34}Fe_{1.62}O_4$	0.22
$Zn_{0.02}Mn_{0.46}Mg_{0.79}Fe_{1.62}O_4$	0.21
$Zn_{0.08}Mn_{0.64}Mg_{0.28}Fe_{1.74}O_4$	0.23
$Zn_{0.18}Mn_{0.57}Mg_{0.16}Fe_{1.79}O_4$	0.33
$Zn_{0.69}Ni_{0.29}Fe_{1.98}O_4$	0.25
(1/8 mil permalloy tape)	0.2
$Y_3Fe_5O_{12}$ (garnet)	0.30

Table IV. Switching Coefficients S_{w_2} (4).

Set	Ferrite Symbol	Core Number	Core Length l	Core Height h	Ratio $\frac{\text{height}}{\text{width}}$
1	F_4	A-1	0.238mm ±3.4%	(circular)	1.0
1	F_4	A-2	0.173mm ±5.9%	0.249mm ±4.1%	1.44
1	F_4	A-3	0.123mm ±7.2%	0.370mm ±2.7%	3.0
2	F_5	B-1	0.198mm ±3.8%	0.218mm ±3.5%	1.1
2	F_5	B-2	0.122mm ±8.3%	0.370mm ±2.7%	3.0
3	F_1	C-1	0.197mm ±3.9%	0.199mm ±3.8%	1.0
3	F_1	C-2	0.104mm ±8.5%	0.375mm ±2.0%	3.7
4	F_5	D-1	0.217mm ±4.7%	0.212mm ±3.0%	1.0
4	F_5	D-2	0.119mm ±10.6%	0.368mm ±2.1%	3.1

Table V. Dimensions of Cores Used to Examine the Dependence of the Flux Switching Mechanism on Core Geometry.

Figure 1. The Spiral Model (5)

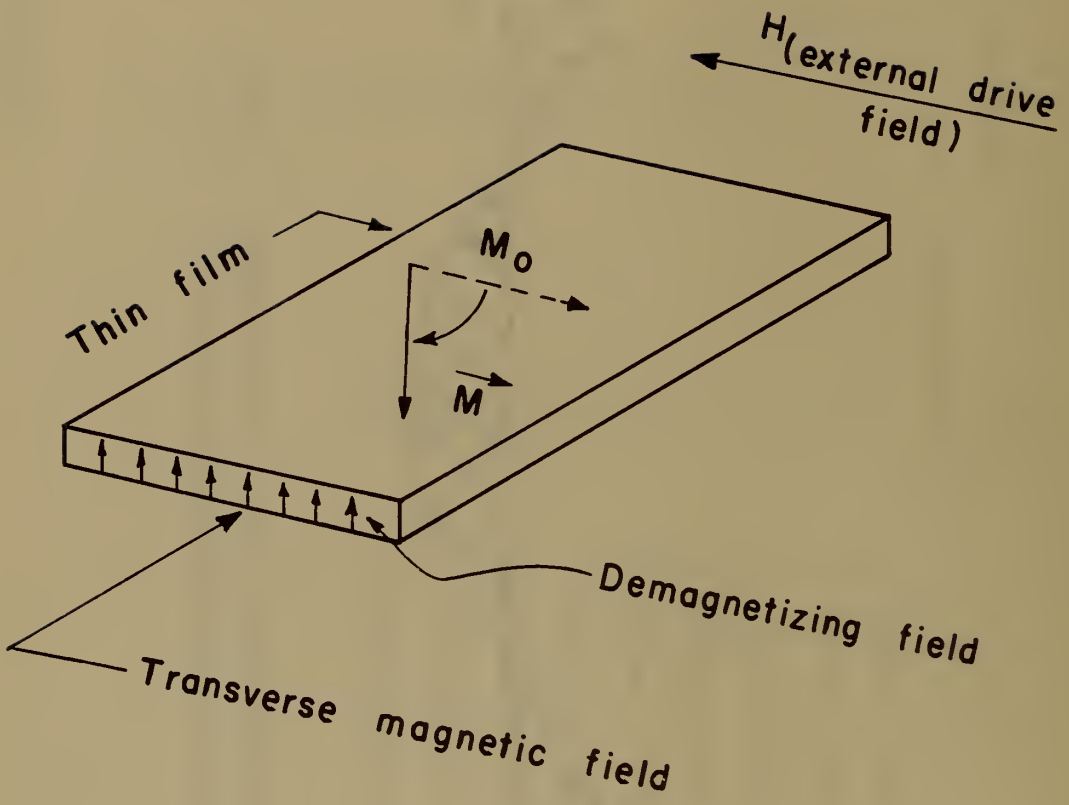

Figure 2. Flux Reversal in Thin Films by Coherent Rotation

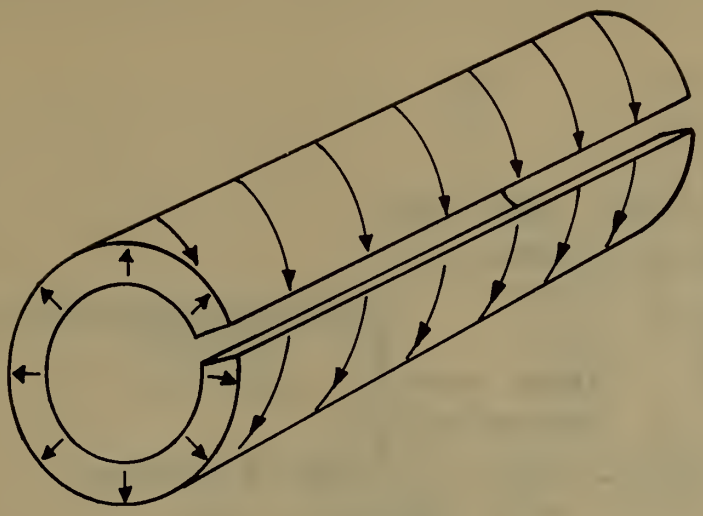

Figure 3. Appearance of the Film in Figure 2 when Wrapped up to Form a Hollow Cylinder

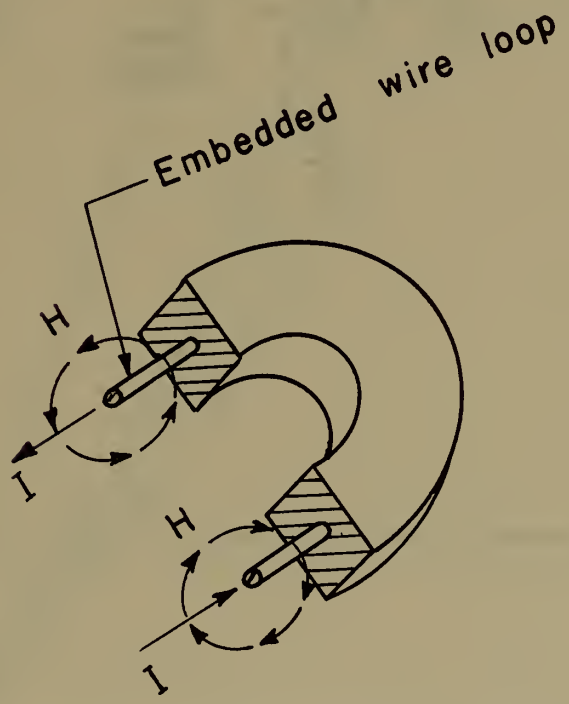

Figure 4. Assumed Cross Section of Core Used to Demonstrate the Coherent Rotational Model in Ferrite Toroids

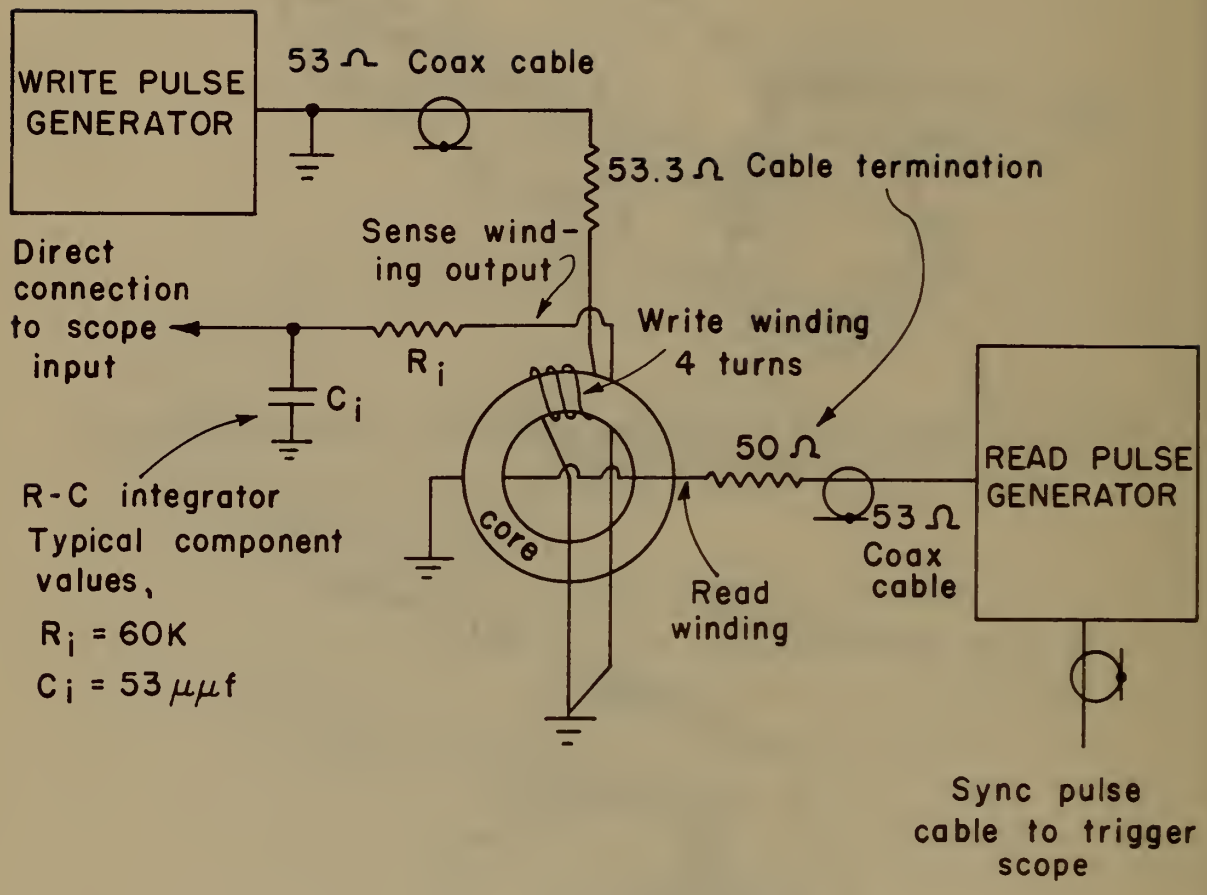

Figure 5. Experimental Layout for Obtaining Switching Curve Data

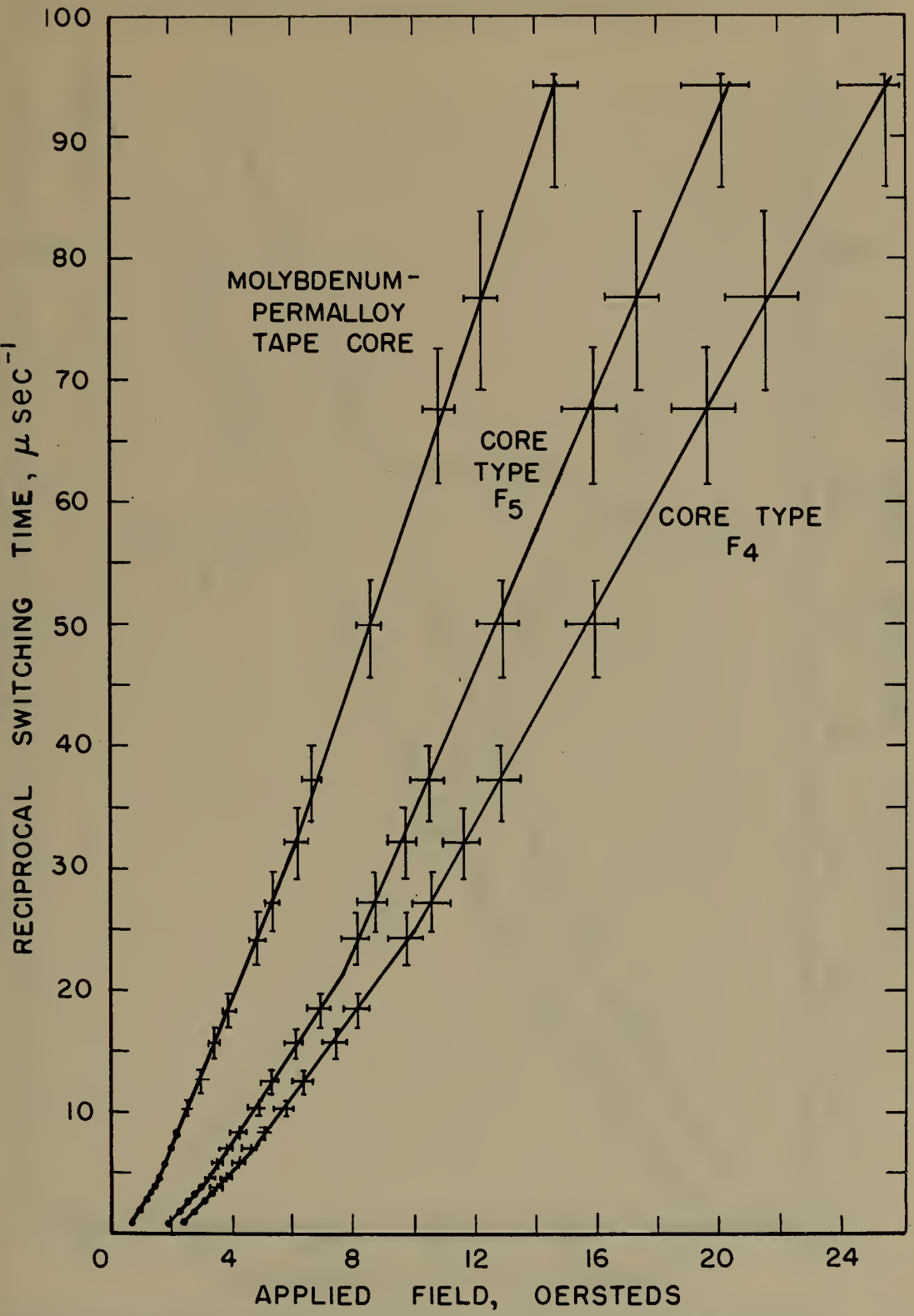

Figure 6. Reciprocal Switching Time Versus Applied Field for a Ferromagnetic Tape Toroid and Ferrite Core Types F_4 and F_5

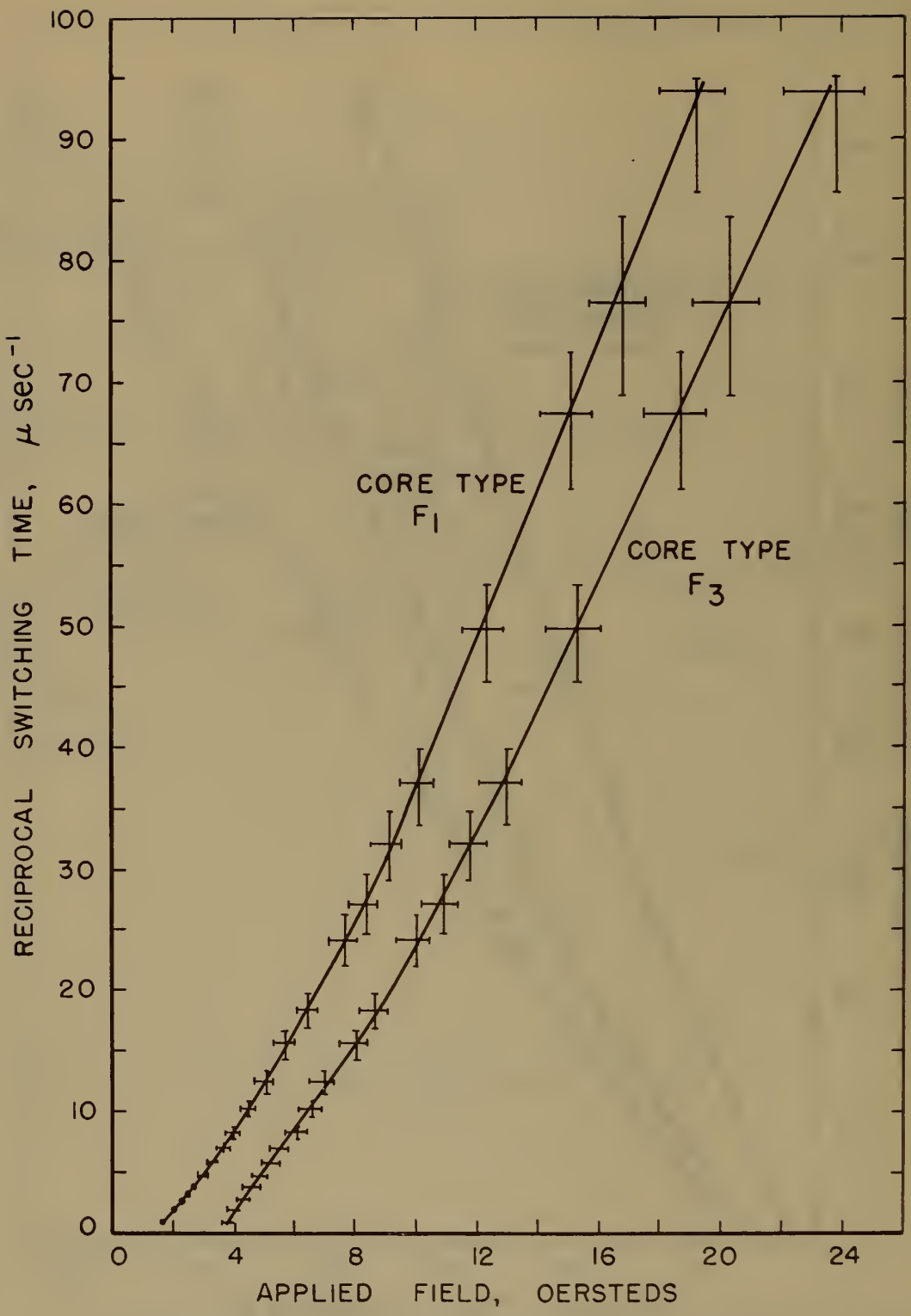

Figure 7. Reciprocal Switching Time Versus Applied Field for Core Types F_1 and F_3

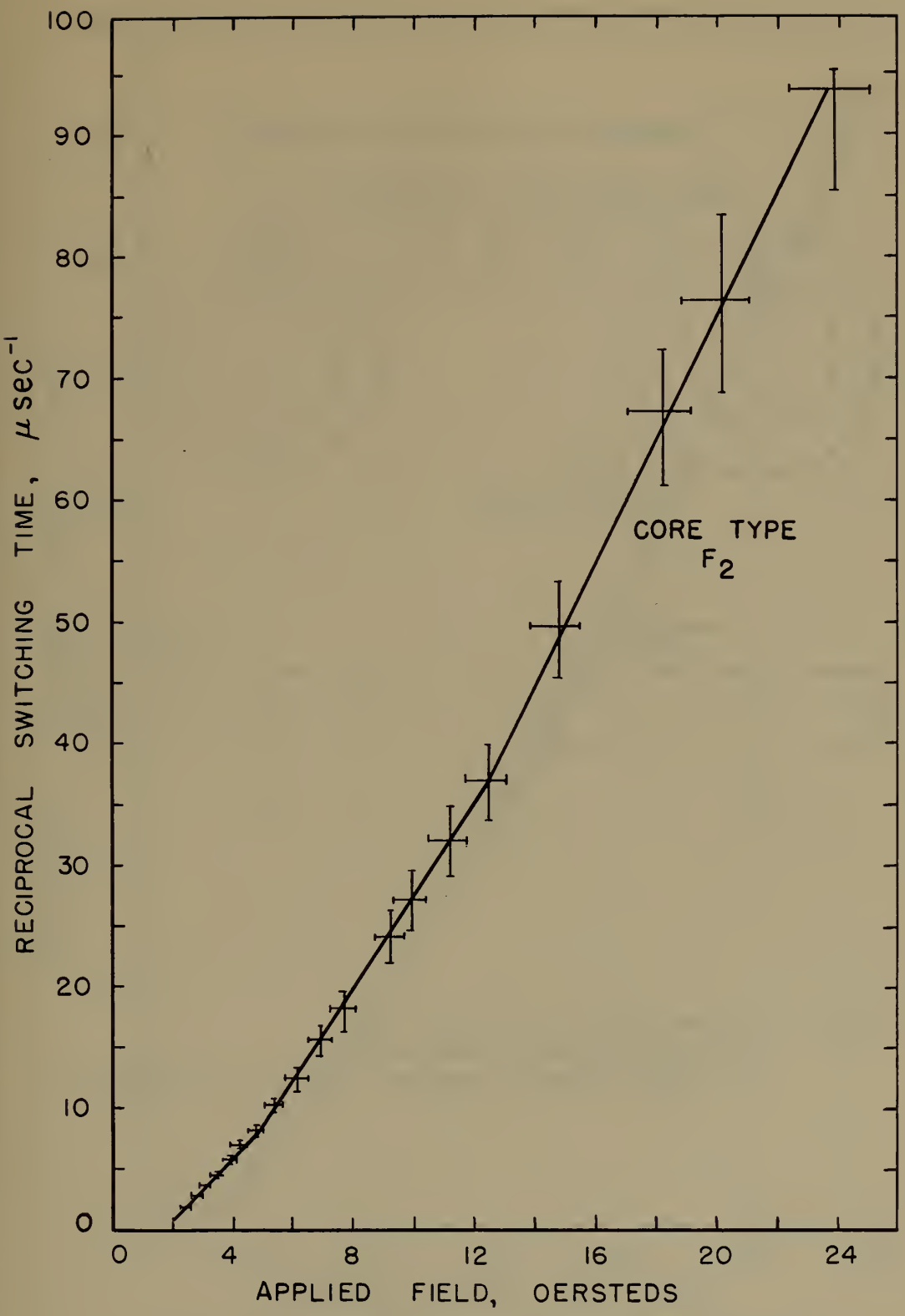

Figure 8. Reciprocal Switching Time Versus Applied Field for Ferrite Core Type F_2

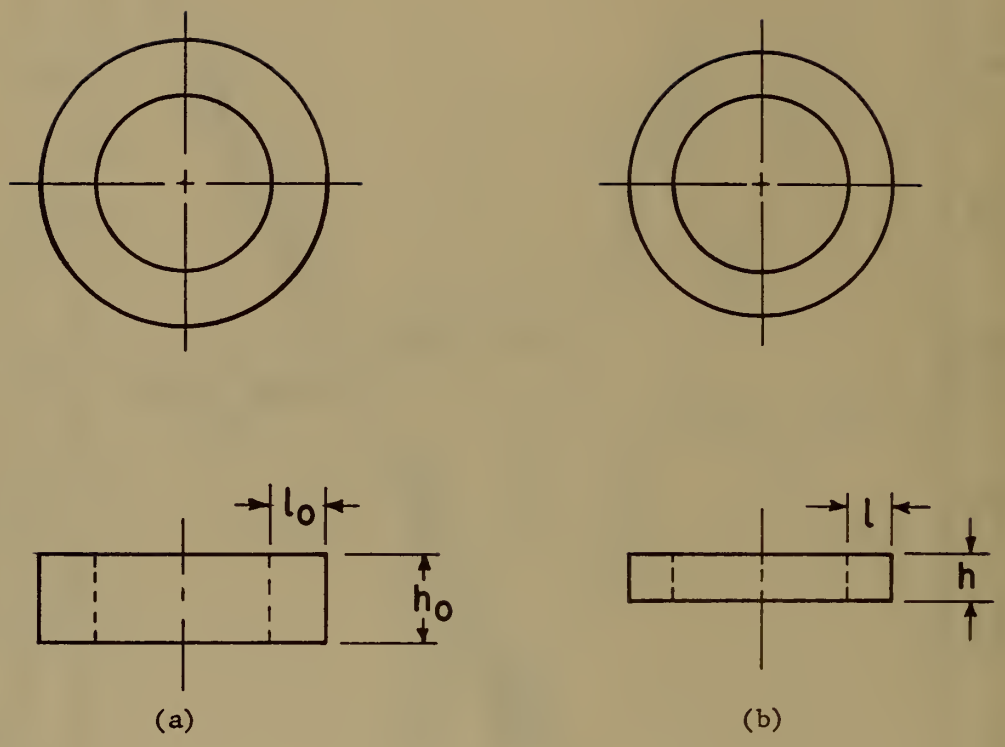

Figure 9. Appearance of a Ferrite Core
(a) As Received Commercially
(b) After Being Ground into a Square Cross Section

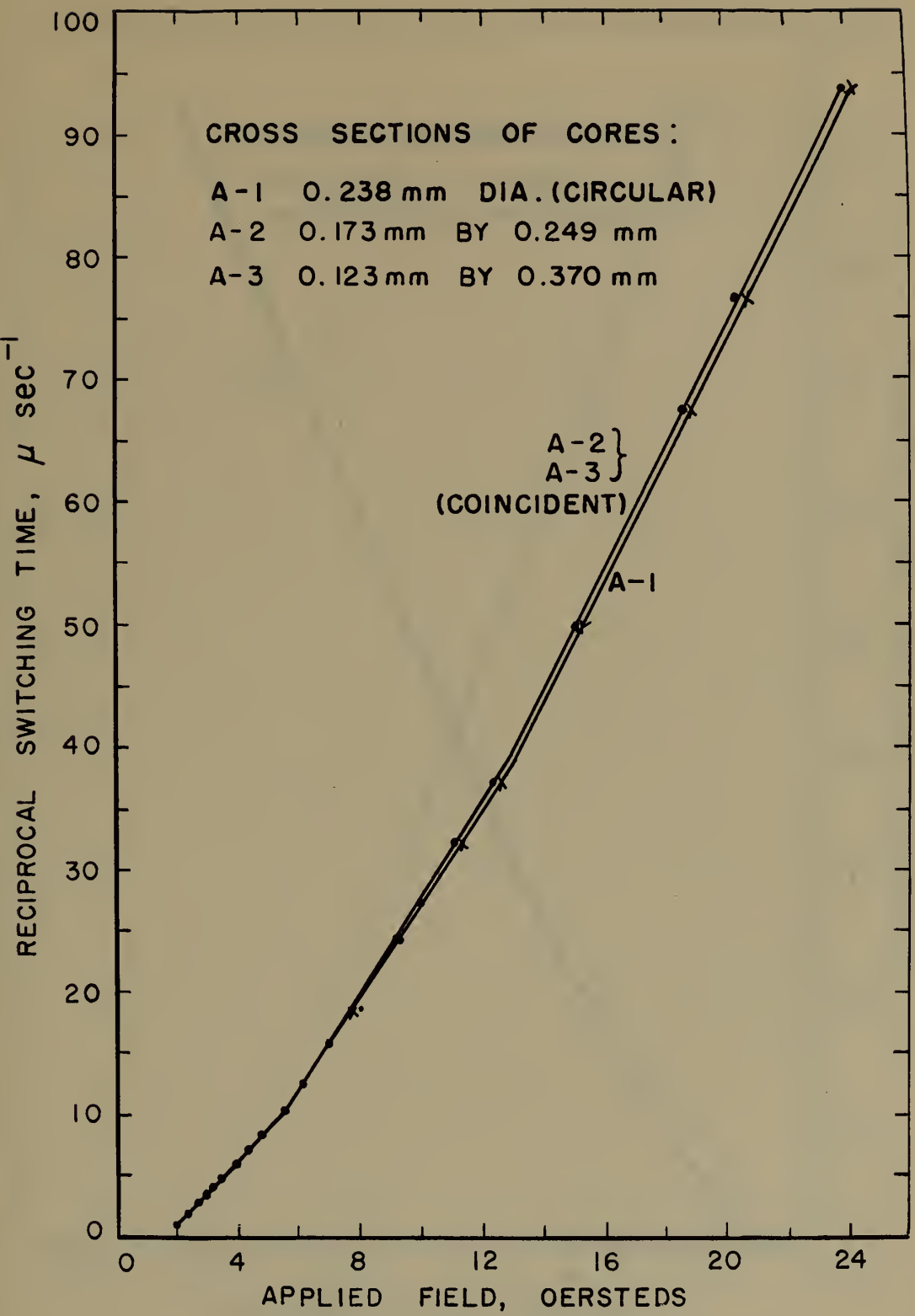

Figure 10. Reciprocal Switching Time Versus Applied Field for 3 Type F_4 Cores of Different Cross Section

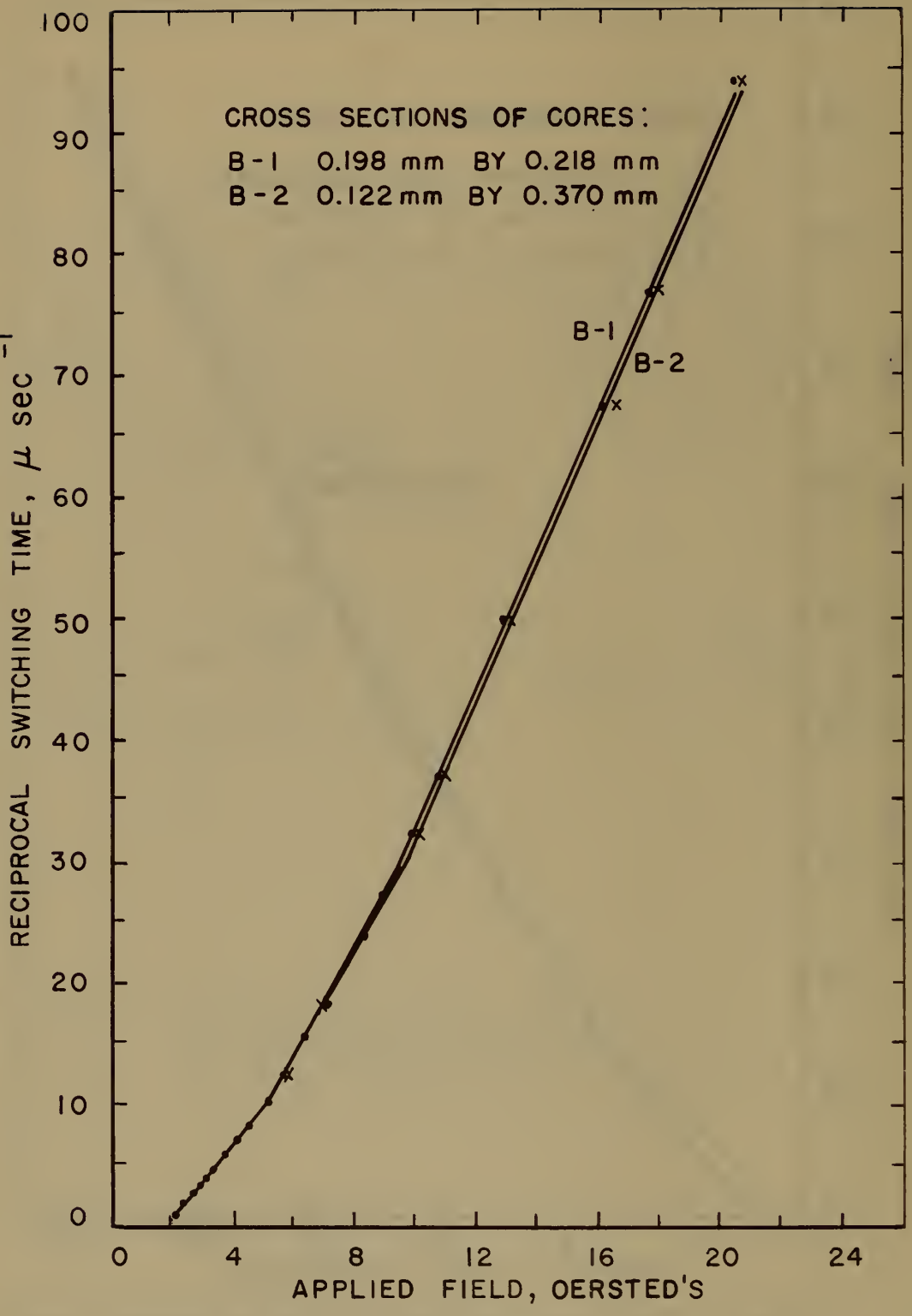

Figure 11. Reciprocal Switching Time Versus Applied Field for 2 Type F_5 Cores of Different Cross Section

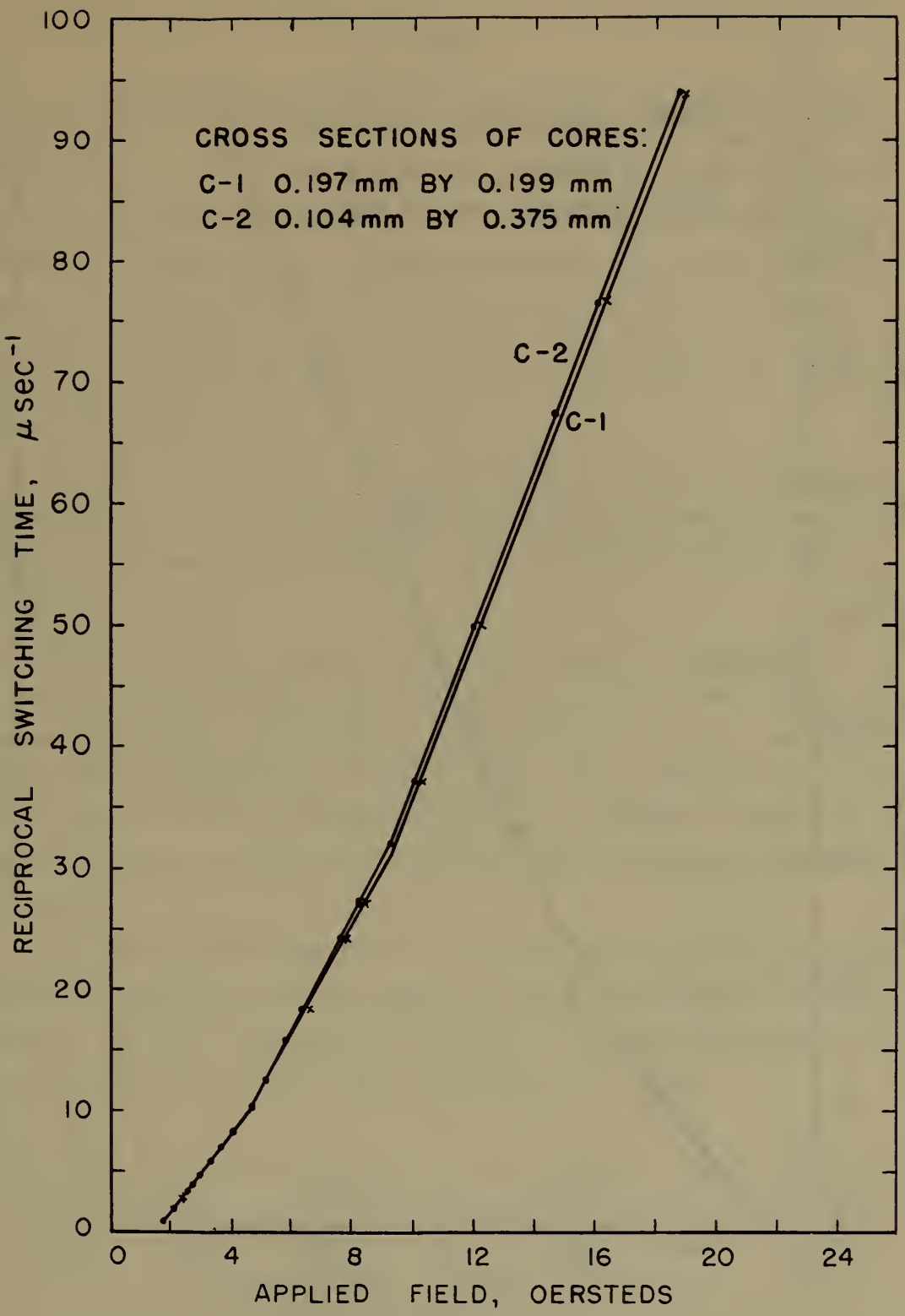

Figure 12. Reciprocal Switching Time Versus Applied Field for 2 Type F_1 Cores of Different Cross Section

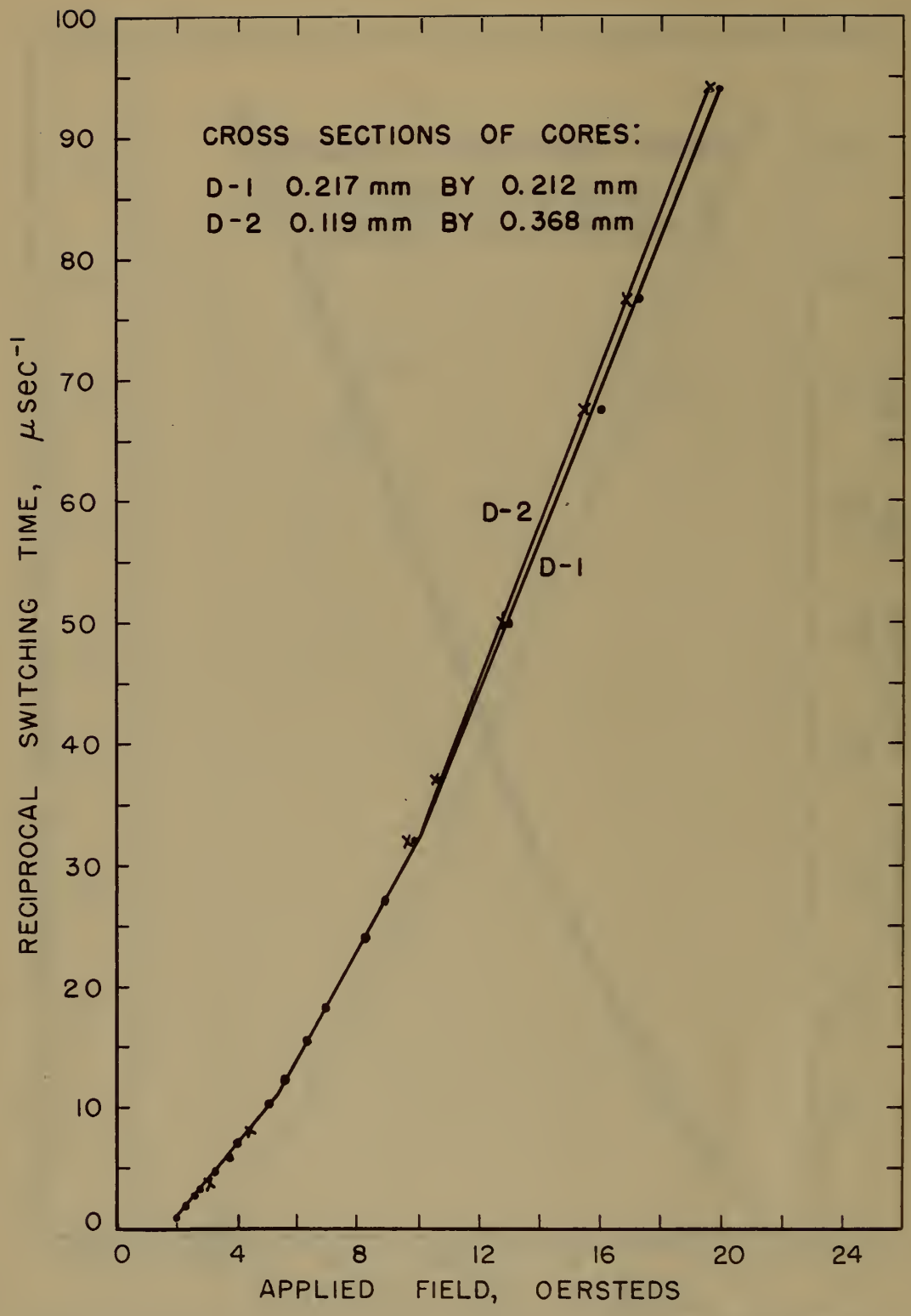

Figure 13. Reciprocal Switching Time Versus Applied Field for 2 Type F_5 Cores of Different Cross Section

APPENDIX

An extension of the switching curves into the region of long write pulses - i.e., those > 1 μsec, was made for core types F_4, F_1, and F_5. In each case, the straight line region corresponding to flux reversal by domain wall motion was extended until a certain value of H was reached, following which no more than 90% of the total irreversible flux could be switched no matter how long the write pulse was made. Presumably, the field at the outermost regions of the core had fallen below the coercive force for the ferrite material.

Figures 14 and 15 show the switching curves for all the core types which were examined. No experimental errors are noted. Figure 14 shows a more detailed view of the lower region of the switching curves.

Figure 14 also reveals that there is usually a straight line transition region between what has previously been referred to in this investigation as the first 2 switching modes - i.e., domain wall motion and incoherent rotation. Various possibilities exist as to the cause for this transition region; for example, it may be a result of flux reversal by both domain wall motion and incoherent rotation.

Two new types of 50-30-15 mil cores were received recently. They are designated as core types F_6 and F_7, and their switching curves are shown in Figures 14 and 15. The switching coefficients were found to be the following, in units of oe - μsec.

Core Type	Sw_1	Sw_2	Sw_3
F_6	0.29	0.19	0.15
F_7	0.50	0.30	0.21

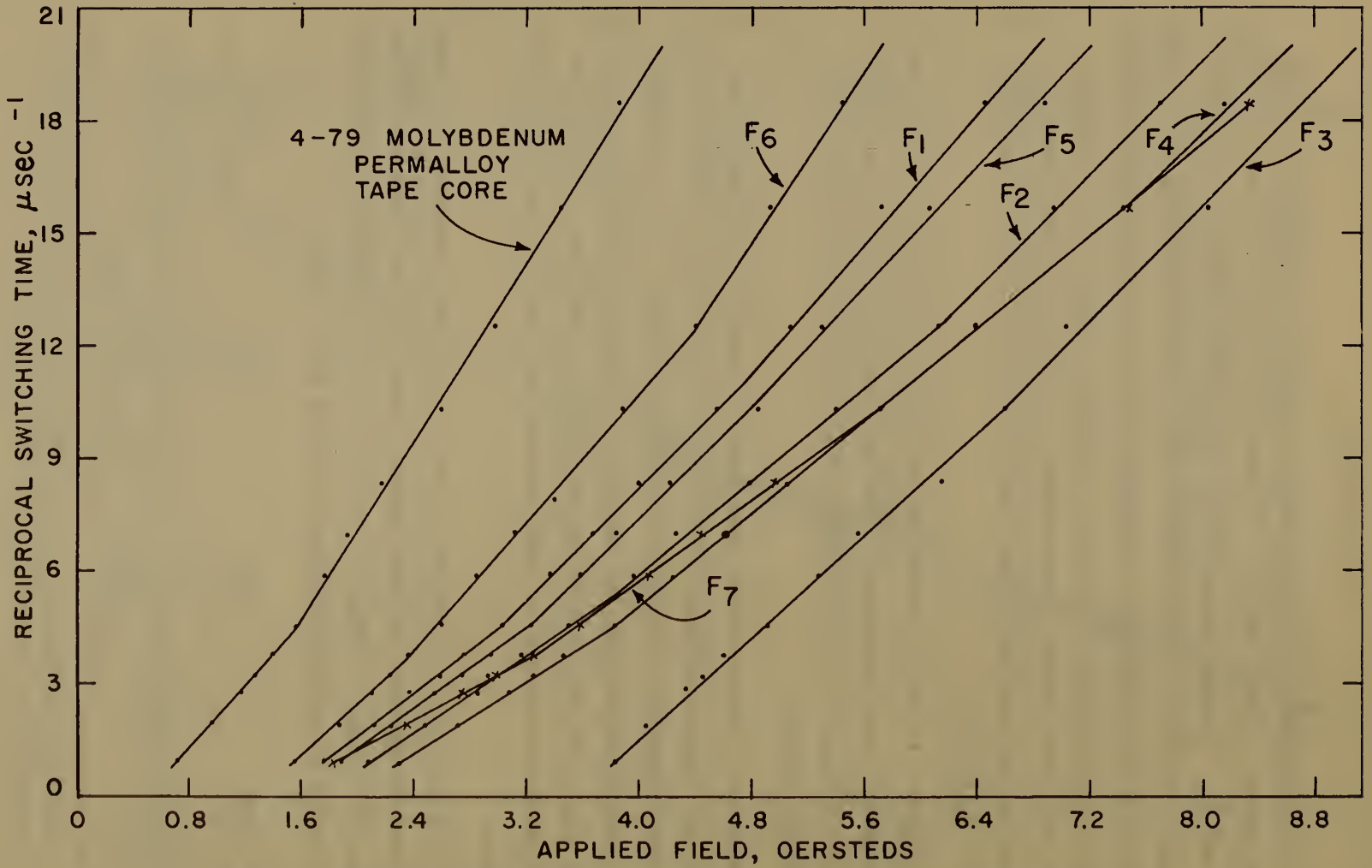

Figure 14. Reciprocal Switching Time Versus Applied Field for Various Ferrite Cores, and for a Permalloy Core

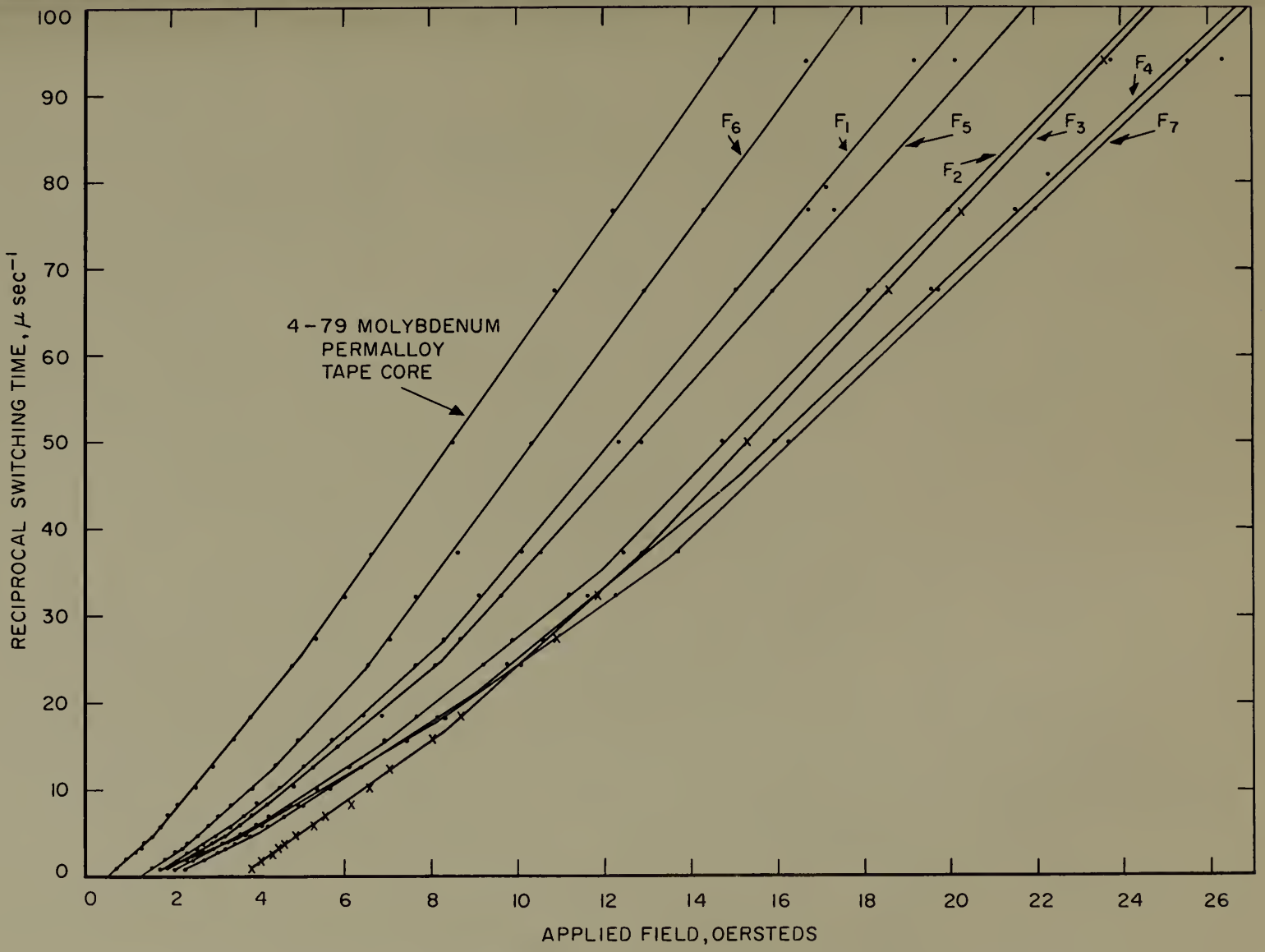

Figure 15. Reciprocal Switching Time Versus Applied Field for a Ferromagnetic Tape Toroid and for Various Ferrite Core Types, as Indicated

U. S. DEPARTMENT OF COMMERCE
Luther H. Hodges, *Secretary*

NATIONAL BUREAU OF STANDARDS
A. V. Astin, *Director*

THE NATIONAL BUREAU OF STANDARDS

The scope of activities of the National Bureau of Standards at its major laboratories in Washington, D.C., and Boulder, Colorado, is suggested in the following listing of the divisions and sections engaged in technical work. In general, each section carries out specialized research, development, and engineering in the field indicated by its title. A brief description of the activities, and of the resultant publications, appears on the inside of the front cover.

WASHINGTON, D.C.

Electricity. Resistance and Reactance. Electrochemistry. Electrical Instruments. Magnetic Measurements. Dielectrics.

Metrology. Photometry and Colorimetry. Refractometry. Photographic Research. Length. Engineering Metrology. Mass and Scale. Volumetry and Densimetry.

Heat. Temperature Physics. Heat Measurements. Cryogenic Physics. Equation of State. Statistical Physics.

Radiation Physics. X-ray. Radioactivity. Radiation Theory. High Energy Radiation. Radiological Equipment. Nucleonic Instrumentation. Neutron Physics.

Analytical and Inorganic Chemistry. Pure Substances. Spectrochemistry. Solution Chemistry. Analytical Chemistry. Inorganic Chemistry.

Mechanics. Sound. Pressure and Vacuum. Fluid Mechanics. Engineering Mechanics. Rheology. Combustion Controls.

Organic and Fibrous Materials. Rubber. Textiles. Paper. Leather. Testing and Specifications. Polymer Structure. Plastics. Dental Research.

Metallurgy. Thermal Metallurgy. Chemical Metallurgy. Mechanical Metallurgy. Corrosion. Metal Physics.

Mineral Products. Engineering Ceramics. Glass. Refractories. Enameled Metals. Crystal Growth. Physical Properties. Constitution and Microstructure.

Building Research. Structural Engineering. Fire Research. Mechanical Systems. Organic Building Materials. Codes and Safety Standards. Heat Transfer. Inorganic Building Materials.

Applied Mathematics. Numerical Analysis. Computation. Statistical Engineering. Mathematical Physics.

Data Processing Systems. Components and Techniques. Digital Circuitry. Digital Systems. Analog Systems. Applications Engineering.

Atomic Physics. Spectroscopy. Radiometry. Solid State Physics. Electron Physics. Atomic Physics.

Instrumentation. Engineering Electronics. Electron Devices. Electronic Instrumentation. Mechanical Instruments. Basic Instrumentation.

Physical Chemistry. Thermochemistry. Surface Chemistry. Organic Chemistry. Molecular Spectroscopy. Molecular Kinetics. Mass Spectrometry. Molecular Structure and Radiation Chemistry.

• Office of Weights and Measures.

BOULDER, COLO.

Cryogenic Engineering. Cryogenic Equipment. Cryogenic Processes. Properties of Materials. Gas Liquefaction.

Ionosphere Research and Propagation. Low Frequency and Very Low Frequency Research. Ionosphere Research. Prediction Services. Sun-Earth Relationships. Field Engineering. Radio Warning Services.

Radio Propagation Engineering. Data Reduction Instrumentation. Radio Noise. Tropospheric Measurements. Tropospheric Analysis. Propagation-Terrain Effects. Radio-Meteorology. Lower Atmosphere Physics.

Radio Standards. High Frequency Electrical Standards. Radio Broadcast Service. Radio and Microwave Materials. Atomic Frequency and Time Interval Standards. Electronic Calibration Center. Millimeter-Wave Research. Microwave Circuit Standards.

Radio Systems. High Frequency and Very High Frequency Research. Modulation Research. Antenna Research. Navigation Systems. Space Telecommunications.

Upper Atmosphere and Space Physics. Upper Atmosphere and Plasma Physics. Ionosphere and Exosphere Scatter. Airglow and Aurora. Ionospheric Radio Astronomy.


NBS